Practical Battery Arc Flash Models

David Rosewater, *Senior Member, IEEE*, Lloyd B. Gordon, *Life Senior Member, IEEE*, and William Cantor, *Senior Member, IEEE*

***Abstract*—Calculating arc flash incident energy (IE) in battery systems can be significantly improved in both accuracy and practicality. Annex D of NFPA 70E has referenced the maximum power transfer method since 2012, which tends to overestimate IE and has led to the overprescription of personal protective equipment for over a decade. Many alternative methods have been proposed but have been either impractical or inaccurate. This confluence of factors means that many battery systems either do not have arc flash labels or are labeled with an arc flash hazard that, if true, would make regular maintenance tasks impractical. This paper develops a practical battery arc flash model that accounts for electrode erosion and self-extinguishing phenomena in different configurations to predict IE. Self-extinguishing time is predicted by modeling the arc length as a random variable and assuming that the arc will extinguish whenever it exceeds a maximum threshold. The probability distribution of the arc length depends on the electrode configuration and the voltage. The proposed method is substantially more accurate than established methods when they are used to predict the IE measured in 228 battery arc flash tests from published literature. This achievement represents a milestone in battery arc flash modeling that will enable appropriate safety controls to be applied to battery work.**

***Index Terms*—Risk assessment, energized work, batteries, work practices, workplace safety.**

I. Introduction

THE physics of an electric arc is extremely complex. However, electrical safety requires simple rules and guidelines to protect workers. If a model is too complex, it will not be widely used. If a model is not precise enough, then it will lead to either the over prescription of controls or electrical injury. This paper attempts to strike a balance between simplicity and precision in calculating battery arc flash incident energy (IE). The goal of this paper is to provide a practical way to calculate battery arc flash IE with the information available to a battery worker. This work builds on a paper presented at the 2025 IEEE IAS ESW [1].

Received 25 March 2025; revised 2 October 2025; accepted 16 October 2025. Date of publication 26 November 2025; date of current version 15 May 2026. Paper 2025-ESafC-0454.R1, presented at the 2025 IEEE IAS Electrical Safety Workshop, Jacksonville, FL, USA, Mar. 3–7, and approved for publication in the IEEE Transactions On Industry Applications by the Electrical Safety Committee of the IEEE Industry Applications Society [DOI: 10.1109/ESW58401.2025.11159144]. This work was work supported by the U.S. Department of Energy, Office of Electricity (OE), ES Division. *(Corresponding author: David Rosewater).*

David Rosewater is with Sandia National Laboratories Albuquerque NM 87111 USA (e-mail: dmrose@sandia.gov).

Lloyd B. Gordon is with Specialized Electrical Safety Services Los Alamos NM 87544 USA.

William Cantor is with the TPI Engineering Exton PA 17349 USA.

Color versions of one or more figures in this article are available at https://doi.org/10.1109/TIA.2025.3637673.

Digital Object Identifier 10.1109/TIA.2025.3637673

With the proliferation of batteries needed for grid scale energy storage it is important to protect battery workers from electrical hazards. Battery arc flash injuries have historically been rare and are difficult to disaggregate from contact thermal injuries in accident data [2]. However, national worker safety standards require arc flash hazard labels on stationary battery systems [3]. The prevailing method to calculate IE in batteries has been the maximum power transfer method described in an informative annex of NFPA 70E [3]. Part of the motivation of this paper is that this method is known to overestimate the IE in battery systems leading to the overprescription of personal protective equipment (PPE). While rare, it can also underestimate the IE in cases where the arc current is lower than expected, leading to slower overcurrent protection and hence longer arc duration. More accurate methods have been developed [4], that can provide a better initial estimate of arc current and hence arc time where overcurrent protection is the limiting factor. However, there is a growing body of experimental evidence that self-extinguishing is the primary limiter of arc duration under certain conditions. This paper explores what these conditions may be and develops a model to predict self-extinguishing time.

The remainder of this paper is organized as follows: The relevant physics of electric arcs in air produced by batteries are reviewed in Section II, the published body of experimental data of battery arc flash is reviewed and categorized in Section III. Methods of dc arc flash calculation, including the novel methods developed for battery arc flash in this paper, are covered in Section IV, and lastly the results of using these methods to predict IE from arc flash tests is presented in Section V.

II. Arc Flash Physics

An electric arc is a continuous discharge of electricity through air that produces light and heat. It occurs when a high voltage is applied across a gap between two electrodes, ionizing the gas and creating a conductive plasma channel. The plasma loses heat rapidly through thermodynamic heat transfer. The arc, therefore, can only sustain itself when the electrical heat generation exceeds the heat dissipation. An electric arc is a continuous discharge of electricity through air that produces light and heat. It occurs when voltage is applied across a gap between two electrodes, ionizes the gas and creates a conductive plasma channel. The plasma transfers heat rapidly through thermodynamic processes. The arc sustains itself when the electrical heat generation exceeds the heat dissipation. There are two stable operating temperatures for electric arcs: where heat generation is balanced by conduction losses (to both the surrounding air and the electrodes), and where it is balanced by

© 2025 The Authors. This work is licensed under a Creative Commons Attribution 4.0 License. For more information, see https://creativecommons.org/licenses/by/4.0/

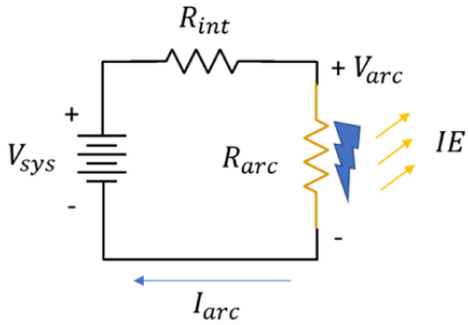


Fig. 1. Battery Arc Flash Hazard Diagram.

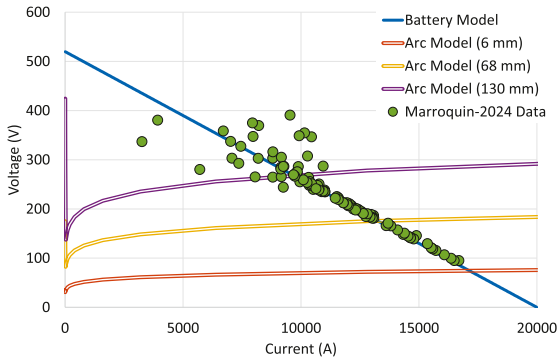


Fig. 2. Battery Arc Flash I-V Data, collected by [9] and presented in [8].

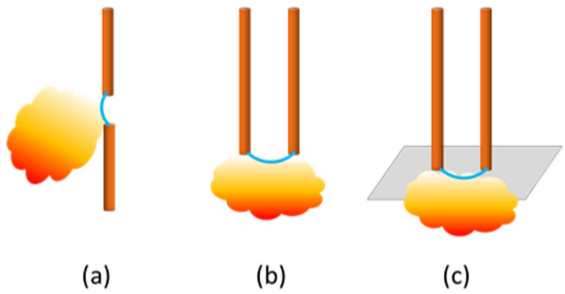


Fig. 3. DC Electrode Configurations: (a) inline, (b) open parallel, (c) closed parallel.

radiation losses. Conduction heat transfer is proportional to the temperature difference and its associated stable temperature is around 6000 K [5]. Radiation heat transfer is proportional to the temperature difference to the fourth power, and its associated stable temperature is much higher around 9000 K [5]. We are primarily concerned with the higher temperature arcs as these are more hazardous to workers [6].

Instead of delving into the complex models of plasma physics, we will look at an electric arc as a simple intersection of two equations: a Thévenin equivalent battery model, and a average power arc model. The IE calculation method developed by Ammerman [4] using the Stokes and Oppenlander [5] model is used in this paper. A diagram of a Thévenin battery model connected to a nonlinear arc resistance model is shown in Fig. 1. This method sets the battery terminal voltage equal to the arc voltage through (1). This equation is solved iteratively by changing the arc current using the goal seek function in MS Excel. A spreadsheet with a macro to solve this function for I_{arc} and V_{arc} is available [7]. Once solved, the arc voltage, current, time, and working distances are plugged into (2) to determine the IE. The relationship in (2) assumes that the arc is at thermal equilibrium, in that the heat gained by the electrical power of the arc is immediately lost by the arc through thermal radiation.

$$V_{\text{arc}} = (20 + 0.534 z_{\text{g}}) I_{\text{arc}}^{0.12} = V_{\text{sys}} - I_{\text{arc}} R_{\text{int}} \tag{1}$$

$$IE = \frac{0.239 \left(\frac{\text{cal}}{\text{J}}\right)}{4\pi D^2} \int_0^{T_{\text{arc}}} V_{\text{arc}}(t) I_{\text{arc}}(t) dt \tag{2}$$

where V_{arc} is the arc voltage (V), I_{arc} is the arc current (A), T_{arc} is the arc time (s), V_{sys} is the battery voltage (V), R_{int} is the battery internal resistance (Ω), z_{g} is the electrode gap (mm), D is the working distance (cm), and IE is the incident energy (cal/cm^2)

In general, (1) approximates the arc's average power as a function of arc gap and arc current. Similar to Ammerman [4], this model is extended to represent a stable voltage and current around which an arc operates. Fig. 2 shows current and voltage data collected during inline arc flash experiments on a 520 V battery with a short circuit current of 20 kA. The initial electrode gap was 6 mm. After two seconds the electrodes had burned back to 130 mm. As shown in the I-V data, the stable voltage-current starts at the intersection of the battery model and the 6 mm arc model. As the test progresses, the measured voltage rises and current falls along the battery model line. At the end of the test, the voltage and current start to behave more erratically, jumping above and below the battery model line. This is likely an artifact of the method of extracting data from the plots in [8] as the raw data was not published along with their paper.

III. Experimental Data

Recent work has surveyed the history of dcarc flash testing [10]. In this paper, an expanded list of references is examined to compare their methodologies and results. The drawings in Fig. 3 show the range of different test configurations used in published works, with the addition of a box in many tests to simulate the arc occurring within an electrical equipment enclosure. Note that of the tests in the literature with a real battery, or a simulated battery with calibrated voltage droop, used as the power source, all tests were performed with low inductance circuits starting with the battery at rest. This is a good match to our assumed linear battery model but it would not apply to other power sources (PV or electronics) or to panels located far from the batteries with long twisted current carrying wires that would store additional energy in their inductance.

The configurations are divided into three categories: inline, open parallel, and closed parallel. The terminology of open (a.k.a. 'unbounded', or 'in open air') and closed (a.k.a. 'terminated in an insulating barrier, or 'butted into a boundary') is used for convenience and does not refer to the enclosure's door position. Due to the high arcing currents of interest, convective forces can be safely ignored meaning that the orientation of the electrodes is not needed to model the arc. The inline configurations have the current carrying conductors in the same line as the arc. This means that the magnetic forces do not impact the arc until it moves outside of this line, at which point the direction of Lorentz forces is in a circle around the conductors as dictated by

the right-hand rule. The parallel configurations have the current carrying conductors oriented parallel to each-other. This means that the magnetic forces project the arc away from the source of energy, no matter the polarity of the electrodes. The open parallel configuration allows the arc to be projected past the length of electrodes while the closed parallel configuration terminates the electrodes in an insulating barrier.

A. Inline Configurations

Inline configurations (Fig. 3(a)) were included in the tests performed in [9], [11], [12], [13], [14], [15]. The data provided in [9], [11], [12], were the most comprehensive as large tables describe every test condition and the results. Data from [13], [14], [15] had to be inferred from the figures. Because of this, some data points from either arc time or incident energy were missing and those tests are omitted. In total, data from 74 arc flash experiments using inline configurations are analyzed in this paper.

These data identify two of the notable phenomena that this paper hopes to address: electrode erosion, and semi-random self-extinguishing time. Electrode erosion, or burn back, has been well documented as important for IE calculation [8] and as a contributing factor for self-extinguishing and is discussed more in Section IV-C. The tests that self-extinguish have a clear trend that higher voltage batteries have longer duration arcs [16] but there is still substantial uncertainty in the arc interrupt time. There was no clear impact of containing the arc within a box on the interrupt time but doing so increased the incident energy measured.

B. Open Parallel Configurations

Parallel configurations without a barrier (Fig. 3(b)) were included in the tests performed in [11], [12], [13], [14], [15]. The spreadsheets in [11], [12], [13] could be read from directly, while data from [14], [15] had to be inferred from the figures. In total, data from 84 arc flash tests using open parallel configurations are analyzed in this paper.

These data show that a battery arc between parallel conductors, without a barrier, is extremely short lived compared with the inline configurations. There is a clear trend that higher voltage leads to a longer arc duration. However, the trend is roughly exponential rather than linear. This phenomenon is governed by the magnetic forces discussed in Section IV-E. Notably, many experimentalists (e.g. Fechalos [12]) started with parallel electrodes to better represent real battery equipment, but changed to inline electrodes when they could not sustain an arc in the parallel configuration.

C. Closed Parallel Configurations

Parallel configurations with a barrier (Fig. 3(c)) were included in tests performed in [13], [17] and [18]. Data from [17] was obtained. Data in [18] did not include any self-extinguishing arcs so could not be used to develop models but could be used to verify model accuracy.

An interesting observation in [13] that adding an isolating barrier to the end of the parallel electrodes extended the arc duration: “Arcs extinguished themselves very quickly when allowed to progress to the top of the bus bars where the arc could expand in free space. A barrier was added to confine the arc to the area between the bus bars. This successfully confined the arc and resulted in longer arc times.” - Hildreth [13]. In total, data from 77 arc flash tests using closed parallel configurations are analyzed in this paper.

Comparing these results to data from [17] complicates this observation. Instead of simply increasing the arc duration, the barrier appears to increase the uncertainty in self-extinguishing time. The arcs were observed to occasionally stretch away from electrodes, perpendicular to the magnetic forces from the electrodes. Identical tests sustained themselves for a duration ranging from several milliseconds to several seconds.

IV. Methods

A. Maximum Power Transfer Method

This is the most widely used method to calculate arc flash IE as it requires the least information. Originally published by Doan in 2007 [19] and later included in Annex D of NFPA 70E [3], this method assumes that the maximum power a dc source is capable of transferring to the arc is 50% of the power delivered by the source and is emitted in all directions as thermal radiation.

$$I_{\text{arc}} = I_{\text{bf}}/2 \tag{3}$$

$$IE \approx 0.01 V_{\text{sys}} I_{\text{arc}} \frac{T_{\text{arc}}}{D^2} \tag{4}$$

where I_{bf} is the bolted fault current.

B. Arc Resistance Method

This method is referenced in NFPA 70E [3], but has seen less wide use than the max power method due to the need to know the arc gap and to iteratively solve for the arc resistance and hence power. This is equivalent to the similar formulation in (1) with the simplifying assumptions of a constant arc gap and known arc duration. First published by Ammerman in 2010 [4], this method calculates the arc resistance at the intersection between the battery’s discharge curve and the arc high-current / low-voltage curve.

$$R_{\text{arc}} = \frac{20 + 0.534 z_g}{I_{\text{arc}}^{0.88}} \tag{5}$$

$$V_{\text{arc}} = V_{\text{sys}} - I_{\text{arc}} R_{\text{int}} \tag{6}$$

$$IE \approx \frac{I_{\text{arc}}^2 R_{\text{arc}} T_{\text{arc}}}{4\pi D^2} \tag{7}$$

One problem with this method is that the arc gap can change over time with electrode erosion. As was shown in Fig. 2 the initial arc gap was below the maximum power point on the battery’s discharge curve. As the arc gap increased, the power increased. So, if the electrode gap is narrower than the max power arc gap, the IE that a worker is exposed to could be between the IE calculated using this method and the maximum power method. Marroquin et al. extended the arc resistance method to predict and account for electrode erosion in IE calculation in [8]. These methods are expounded in the following sections.

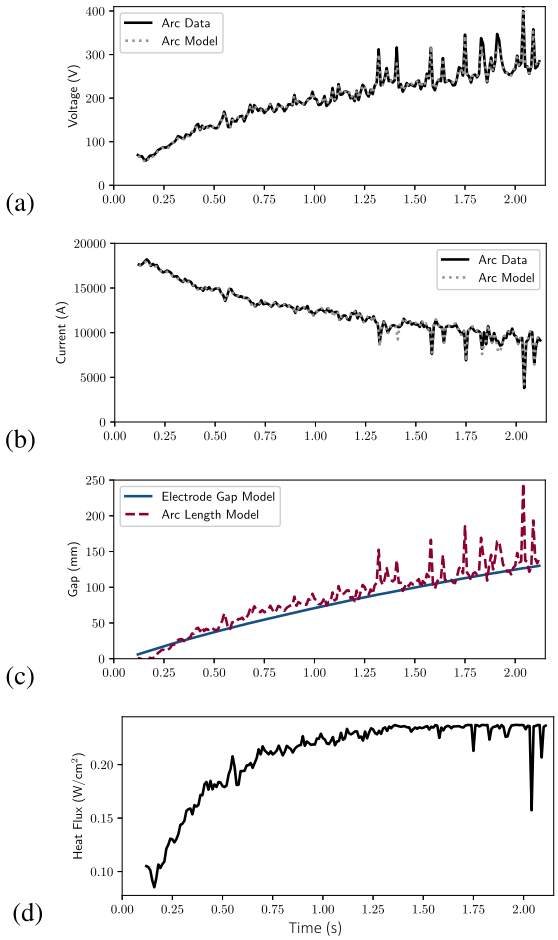


Fig. 4. Arc Model with Electrode Erosion, (a) Arc Voltage, (b) Arc Current, (c) Electrode Gap from (9) and Arc Length from (10), and (d) Arc Heat Flux at an 45 cm (18 in) working distance.

C. Erosion Model

A novel modification of the arc resistance method is developed by determining the rate of electrode erosion. The growth of the electrode gap is a function of the heat generated by the arc, some of which melts or vaporizes the metal of the electrodes. Previous studies have modeled this rate as proportional to current [8], [10], [20]. We attempted to model it as proportional to current squared and arc power and both fit the results when the final arc gap is known. However, when predicting what the final arc gap will be, modeling electrode erosion as proportional to current yields the most accurate results. Hence, the function shown in (8) is used to model arc erosion.

$$\frac{dz_g}{dt} = K_{\mathrm{g}} I_{\mathrm{arc}} \tag{8}$$

where K_{g} is the arc erosion rate constant (mm A^{-1} s^{-1})

The erosion rate constant of the experiment is calculated, as shown in Fig. 4, by solving the following multi-objective optimization problem with inputs: V_{arc} arc voltage data, I_{arc} arc current data, $IE = 44$ cal/cm^2 the measured total IE at a working distance D of 45.7 cm, z_0 is the initial electrode gap of 6mm while z_1 is the final electrode gap of 130 mm. The unitless weight Γ is set at 100 to balance how much the optimization tries to fit the I-V data and how much it tries to fit the IE data.

$$\begin{aligned}
\min_{x} \quad & ||V_{\mathrm{arc}} - \hat{\mathbf{v}}_{\mathrm{arc}}||_2^2 + ||I_{\mathrm{arc}} - \hat{\mathbf{i}}_{\mathrm{arc}}||_2^2 + \Gamma \left(\Phi - \sum \hat{\phi}\right)^2 \\
\text{s.t.} \quad & \hat{\mathbf{v}}_{\mathrm{arc}} = V_{\mathrm{sys}} - \hat{\mathbf{i}}_{\mathrm{arc}} R_{\mathrm{int}} \\
& \hat{\phi} = 0.239 \left(\frac{\mathrm{cal}}{\mathrm{J}}\right) \frac{\Delta t \hat{\mathbf{v}}_{\mathrm{arc}} \hat{\mathbf{i}}_{\mathrm{arc}}}{4\pi D^2} \\
& \Xi \hat{\mathbf{z}}_{\mathrm{g}} = K_{\mathrm{g}} \hat{\mathbf{i}}_{\mathrm{arc}} \\
& \hat{\mathbf{z}}_{\mathrm{g}}(0) = z_0 \\
& \hat{\mathbf{z}}_{\mathrm{g}}(n) = z_1
\end{aligned} \tag{9}$$

where $x = \{\hat{\mathbf{v}}_{\mathrm{arc}}, \hat{\mathbf{i}}_{\mathrm{arc}}, \hat{\phi}, \hat{\mathbf{z}}_{\mathrm{g}}, V_{\mathrm{sys}}, R_{\mathrm{int}}, K_{\mathrm{g}}\} \in \mathbb{R}^{4n+3}$. and Ξ is the discrete time matrix:

$$\Xi = \frac{1}{\Delta t} \begin{bmatrix} -1 & 1 & 0 & . & . & 0 \\ 0 & -1 & 1 & 0 & . & . \\ & & . & . & & \\ & & & . & . & \\ 0 & & & 0 & -1 & 1 \end{bmatrix}_{n \times (n+1)}$$

This problem is solved in python using pyomo [21] and the interior point, non-linear solver ipopt. The results are shown in Fig. 4. For the 25 mm diameter copper electrodes used in this experiment Kg = 0.00496 mm A^{-1} s^{-1} . This value is used for tests in [9] and [11]. Fechalos [12] used 19 mm copper electrodes and Hildreth [13] used 14.3 mm copper electrodes so their K_{g} is scaled by the ratio of their cross-sectional areas ($K_{\mathrm{g}} = 0.00855$ mm A^{-1} s^{-1} [11], and 0.01517 mm A^{-1} s^{-1} respectively). Fechalos [12] used 19 mm tungsten electrodes for one test and so we scaled K_{g} by both cross-sectional area and the ratio of density. This calculation resulted in 0.0073 mm A^{-1} s^{-1} for the tungsten electrode test in [12]. Note that trying to adjust for the heat capacity and melting temperature of tungsten produced an inaccurate underestimation of electrode erosion. These are rough approximations and further testing is required to parameterize this phenomenon.

Solving (1) for z_g provides a real-time estimate of the arc length based on the battery model and measured current. This estimate is distinct from the electrode gap burn back in that it comes from the intersection of the battery discharge curve and the arc model.

$$z_{\mathrm{g}} = \frac{V_{\mathrm{sys}} I_{\mathrm{arc}}^{-0.12} - R_{\mathrm{int}} I_{\mathrm{arc}}^{0.88} - 20}{0.534} \tag{10}$$

The arc length estimate, shown in Fig. 4(c), is observed to jump above the electrode gap, peaking above 200 mm. The random behavior of the arc length estimate suggests a method to predict the self-extinguishing time of an arc. If the arc length behaves like a random variable, then the likelihood that, over time, it extends long enough to extinguish itself can be calculated. The following section explores this potential solution.

D. Arc Length as a Random Variable

A clear trend is observable in the experimental data that arcs self-extinguish. Stokes observed the following "... the arc obviously has a tendency to extinguish itself if the source voltage is less than the maximum excursion voltage." [5]. He noted that how often the arc self-extinguished depended on current,

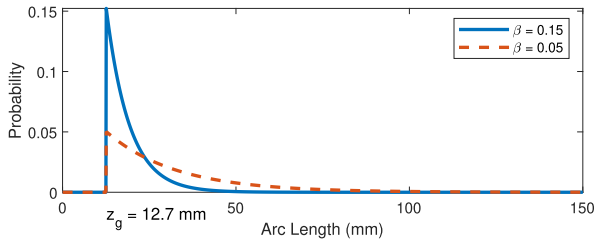


Fig. 5. Example probability distributions for $\tilde{z}$.

with the rate increasing to hundreds of times per second at 1 kA. Our objective is therefor to use what is known about the battery system (voltage, short circuit current, electrode gap, and configuration) to estimate the self-extinguishing time with quantitative accuracy.

To accomplish this goal, the arc length of inline conductors is modeled using a random variable ($\tilde{z}$). The arc length cannot be shorter than the gap between electrodes (z_{g}). We assume that the arc lengths longer than this minimum are exponentially less likely. The probability density function for the arc length based on this assumption is shown in (11).

$$\rho(\tilde{z}) = \beta e^{\beta(z_{\text{g}}-\tilde{z})} \qquad \tilde{z} \in \mathbb{R} \geq z_{\text{g}} \tag{11}$$

where ρ is the probability density function, $\tilde{z}$ is the random arc length which is a real number ($\mathbb{R}$) greater than the electrode gap (z_{g})), and β is a constant describing the distribution with high β corresponding to a short tail (with outcomes tending to be close to z_{g}), and low β corresponding to a long tail (with outcomes tending to be significantly greater than z_{g}). See the parameterization functions in the Appendix. An illustration of two example distributions is shown in Fig. 5.

We assume that the maximum arc length is where there is no solution to (1). The maximum arc length of the arc model in [4] occurs at the transition current between the low-current / high-voltage region, and the low-voltage/high-current region as shown in (12). Plugging (12) into (1) provides (13).

$$I_{\text{t}} = 10 + 0.2 z_g \tag{12}$$

$$(20 + 0.534 z_{\text{g}})(10 + 0.2 z_g)^{0.12} = V_{\text{sys}} - (10 + 0.2 z_g) R_{\text{int}} \tag{13}$$

where I_{t} is the transition current (A).

The solution to (13) yields the self-extinguishing arc length z' for a given battery, above witch no arc can sustain itself [22]. The next step is to calculate β based on measured T_{arc} values in arc flash experiments. The model then uses (11) to predict likelihood of self-extinguish in less than T_{arc} as the probability that $\tilde{z}$ exceeds the arc length limit z' within the time T_{arc}. To integrate $\rho(\tilde{z})$ with respect to time $z_g(t)$ is determined. This will be done in two ways based on the electrode configuration.

For inline configurations, $z_g(t)$ is dominated by electrode erosion as described in (8). However, determining the arc current using (1) is more complex than needed for the assumed linear source. Again, a linear model limits the applicability of this method to batteries (not PV or electronics) and to low-inductance circuits (i.e. on or near the battery itself). With a known final electrode gap (z_1) and arc time T_{arc} this method uses a simple linear approximation for $z_g(t)$ as shown in (14).

$$z_g(t) = z_0 + K_{\text{g}} \int_0^{T_{\text{arc}}} I_{\text{arc}} dt \approx \left(\frac{z_1 - z_0}{T_{\text{arc}}} \right) t + z_0 \tag{14}$$

Plugging the approximation in (14) into (11) and integrating with respect to time yields (15).

$$\rho(\tilde{z}, T_{\text{arc}}) \approx \frac{T_{\text{arc}}}{z_1 - z_0} e^{\beta(z_1 - \tilde{z})} \tag{15}$$

With this result, the probability $\mathbb{P}$ that the random variable $\tilde{z}$ is greater than the maximum arc length z' can be calculated. This is calculated by integrating (15) over the arc length from z' to ∞. The result of this calculation is shown in (16). Equation (16) is then solved for the arc duration T_{arc}, where the probability that the arc self-extinguishes reaches a specified value to produce the time-at-risk equation in (17).

$$\hat{\mathbb{P}}(\tilde{z} \geq z') = \frac{T_{\text{arc}}}{\beta(z_1 - z_0)} e^{\beta(z_1 - z')} \tag{16}$$

$$\hat{T}_{\text{arc}} = \frac{\mathbb{P}(\tilde{z} \geq z') \beta (z_1 - z_0)}{e^{\beta(z_1 - z')}} \tag{17}$$

For each arc flash experiment with a known self-extinguishing time, there exists $\beta \in \mathbb{R}_+$ that solves (17) for values of $\mathbb{P}(\tilde{z} \geq z') \in [0, 1]$. This is to say that we can pick the probability we are interested in, e.g. 50% chance of the arc time exceeding estimate or the median result, and calculate $\beta_{50\%}$ as the tuning parameter to model that outcome. These values are a function of voltage and are listed in the Appendix.

While (17) provides a quantitative estimate for T_{arc}, it requires a known final electrode gap z_1 to calculate. In practice, $\hat{T}_{\text{arc}}$ and $\hat{z}_1$ can be solved together iteratively by approximating I_{arc} and V_{arc} the same as for $z_{\text{g}}(t)$ as shown in (22) and (23). Equations (18) through (21) are simplifying nomenclature.

$$I_0 = I(z_g = z_0) = I(t = 0) \tag{18}$$

$$V_0 = V(z_g = z_0) = V(t = 0) \tag{19}$$

$$I' = I(z_g = z') = I(t = \hat{T}_{\text{arc}}) \tag{20}$$

$$V' = V(z_g = z') = V(t = \hat{T}_{\text{arc}}) \tag{21}$$

$$\hat{V}(t) \approx \frac{V' - V_0}{\hat{T}_{\text{arc}}} t + V_0 \tag{22}$$

$$\hat{I}(t) \approx \frac{I' - I_0}{\hat{T}_{\text{arc}}} t + I_0 \tag{23}$$

$$\hat{z}_1 \approx z_0 + K_{\text{g}} \int_0^{\hat{T}_{\text{arc}}} \hat{I}(t) dt = z_0 + \frac{K_{\text{g}}(I' + I_0)}{2} \hat{T}_{\text{arc}} \tag{24}$$

The time $\hat{T}_{\text{arc}}$ and gap $\hat{z}_1$ are solved for using (17) and (24). Note that many experiments with inline configurations self-extinguish so quickly as to result in no electrode burn back. In these cases, we tend to find $\hat{z}_1 - z_0$ is a fraction of a millimeter. The arc flash IE is estimated by plugging (22) and (23) into (2) and solving the integral. This yields the surprisingly simple formulation in (25). Because it is a functions of the time-at-risk

from (17), (25) is an energy-at-risk (EaR) function

$$\hat{IE} \approx \frac{0.239\left(\frac{\text{cal}}{\text{J}}\right)}{4\pi D^2}\int_0^{\hat{T}_{\text{arc}}} \hat{V}(t)\hat{I}(t)\,dt$$
$$= \frac{0.239}{4\pi D^2}\left(\frac{I'V' + I_0V_0}{3} + \frac{V'I_0 + I'V_0}{6}\right)\hat{T}_{\text{arc}} \quad (25)$$

E. Arc Elongation in Parallel Configurations

In parallel electrode configurations there is a strong magnetic field between the conductors that induces a Lorentz force on the arc plasma. Ampere's law states that the integral of the magnetic field strength (B) around any arbitrary closed loop path is equal to the vacuum magnetic permeability (μ_0) times the enclosed current. A circular path around a wire or electrode has a path length equal to the the circumference of the circle.

$$\oint Bds = \mu_0 I \quad (26)$$

$$B_{\text{wire}}(r)2\pi r = \mu_0 I \;\; \forall r > r_0 \quad (27)$$

$$B_{\text{wire}}(r) = \frac{\mu_0 I}{2\pi r} \;\; \forall r > r_0 \quad (28)$$

where B_{wire} is the magnetic field strength around a wire, r is the radius of the circle centered on the wire, I is the current in the wire, and r_0 is the radius of the wire. Note that bus bar tend to be flat and wide compared to their thickness. For bus bars, we integrate around a roughly rectangular path equidistant from its surface.

$$B_{\text{bus}}(r) = \frac{\mu_0 I}{2h + 2w + 8r} \;\; \forall r > \frac{w}{2} \quad (29)$$

where B_{bus} is the magnetic field strength around a bus bar, h is the height (or thinness) of the bus bar, w is the width of the bus bar, and r is the distance away from the bus bar's center point.

The strength per unit length of the Lorentz force on the arc is the arc current density times the magnetic field strength. However, two additional considerations modify the equations above given the electrode configuration. First, these equations are based on an infinitely long current carrying wire. The arc diverts the current away from the conductor, so the magnitude of the magnetic field is divided by two. Second, there are two wires or bus bars in dc arc flash, hence we include a term for both with different references for r.

$$\frac{dF_{\text{wire}}}{dr} = \frac{\mu_0 I_{\text{arc}}^2}{4\pi}\left(\frac{1}{r} + \frac{1}{2r_0 + z_g - r}\right) \;\; \forall r_0 < r < r_0 + z_g \quad (30)$$

$$F_{\text{wire}} = \frac{\mu_0 I_{\text{arc}}^2}{2\pi}\left(\ln(r_0 + z_g) - \ln(r_0)\right) \quad (31)$$

$$\frac{dF_{\text{bus}}}{dr} = \frac{\mu_0 I_{\text{arc}}^2}{2}\left(\frac{1}{2h + 2w + 8r} + \frac{1}{2h + 10w + 8z_g - 8r)}\right) \;\; \forall \frac{w}{2} < r < \frac{w}{2} + z_g \quad (32)$$

$$F_{\text{bus}} = \frac{\mu_0 I_{\text{arc}}^2}{8}\left(\ln(2h + 6w + 8z_g) - \ln(2h + 6w)\right) \quad (33)$$

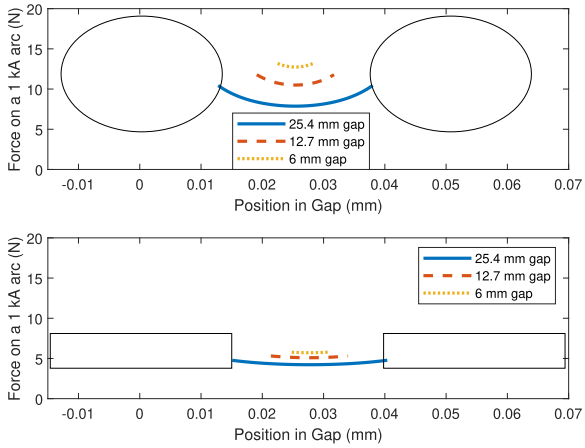


Fig. 6. Initial magnitude of Lorentz force on an 1 kA dc arc, 25.4 mm diameter cylindrical electrodes (top), 8 mm by 30 mm flat bus bars (bottom).

The illustration in Fig. 6 shows how the different electrode shapes and gaps impact the strength of the Lorentz force. The force is stronger on an arc between round electrodes. Further, the gap has a much larger impact on the force for round electrodes than it has on parallel bus bars. However, despite knowing this force, the movement and duration of the arc is complicated by the temperature, density, and mass flow and hence all attempts at incorporating force into a more accurate statistical model of parallel electrode arcs were unsuccessful. The following derivation mirrors the estimation of T_{arc} with the simplifying assumption of constant arc gap (z_g).

Using a constant electrode gap in (11) and integrating with respect to time yields (15). This is then used to calculate the probability $\mathbb{P}$ that the random variable $\tilde{z}$ is greater than the maximum arc length z' causing the arc to self-extinguish. The result of this calculation is shown in (35) which is then solved for the arc duration T_{arc}, where the probability that the arc self-extinguishes reaches a specified value to produce (36).

$$\rho(\tilde{z}, T_{\text{arc}}) \approx T_{\text{arc}} e^{\beta(z_1 - \tilde{z})} \quad (34)$$

$$\hat{\mathbb{P}}(\tilde{z} \geq z') = \frac{T_{\text{arc}}}{\beta} e^{\beta(z_g - z')} \quad (35)$$

$$\hat{T}_{\text{arc}} = \frac{\mathbb{P}(\tilde{z} \geq z')\beta}{e^{\beta(z_g - z')}} \quad (36)$$

V. Results

The goal of this paper is to develop practical methods to calculate battery arc flash hazard. Available to anyone reading this paper [7] is an open-source licensed spreadsheet that is programmed to enable a user to calculate the IE using the methods described in Section IV. With automated calculation, the remaining challenge is in determining accurate inputs. We define the information available to an analyst in two tiers 1) electrical only, and 2) electrical + mechanical. An arc in a box coefficient of 1.52 is used for all experiments performed within enclosed spaces based on the calculated value for panelboards [16], [23].

If all that is known about a battery system is its electrical characteristics, then the only method that can be used in the maximum power transfer method (see Section IV-A). This is

TABLE I
INFORMATION REQUIREMENTS FOR EACH METHOD

	Electrical		Mechanical	
	Battery Voltage	Short Circuit Current	Gap Distance	Electrode Configu-ration
Max-Power	✓	✓		
Arc-Resistance	✓	✓	✓	
Self-Extinguishing	✓	✓	✓	✓+

+ inline configurations also require an assumed erosion rate constant (K_g)

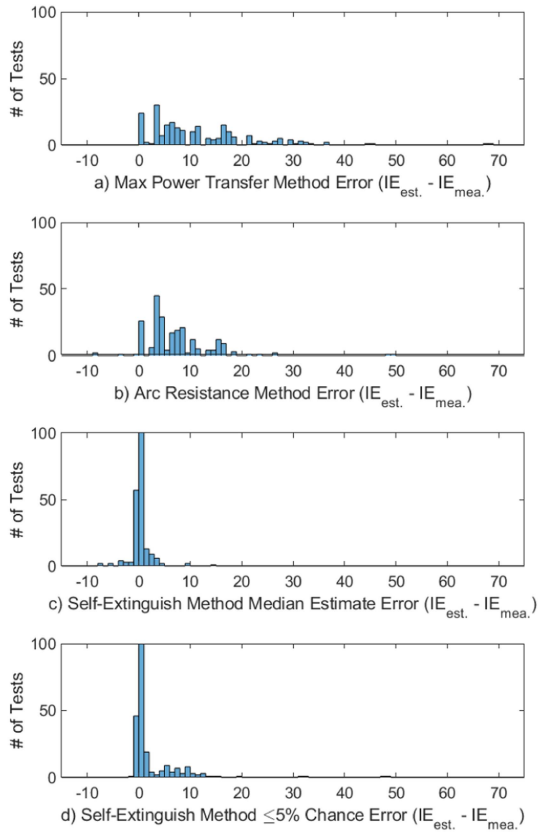


Fig. 7. Prediction error histograms: (a) maximum power method, (b) arc resistance method, (c) median result of the self-extinguish method, and (d) ≤ 5% chance result of the self-extinguish method.

why it is so widely used, despite its tendency to significantly overestimate the level of the hazard. If the mechanical characteristics of a battery system are known, including the configuration and arc gap, then a much more accurate estimate of *IE* can be calculated. The simplest method to account for the arc gap is to use the arc resistance method (see Section IV-B). However, this method ignores how arc gaps can change over time and the propensity of arcs to self-extinguish in different configurations. Table I summarizing the information required to use each IE calculation method discussed in this paper.

The proposed method to account for these phenomena is the self-extinguishing method, which combines electrode erosion (see Section IV-C), and arc length as a random variable (see Section IV-D). Fig. 7 shows histograms of the error from using these three methods to predict the *IE* of 228 tests (see Section III). The self-extinguishing method results are divided between the median estimate c), and the EaR estimate d) where there is a less than 5% chance that the *IE* is higher than the

TABLE II
RESULTS BY ARC FLASH PPE CATEGORY

Method Predicts Correct PPE Category	Max Power	Arc Resistance	SE Median	SE ≤5% EaR
Number	26	28	192	153
%	11.4%	12.3%	84.2%	67.1%

Method Predicts Higher PPE Category	Max Power	Arc Resistance	SE Median	SE ≤5% EaR
Number	202	198	8	74
%	88.6%	86.8%	3.5%	32.5%

Method Predicts Lower PPE Category	Max Power	Arc Resistance	SE Median	SE ≤5% EaR
Number	0	2	28	1
%	0.0%	0.9%	12.3%	0.4%

Number is out of 228 tests.

Error Summary	Max Power	Arc Resistance	SE Median	SE ≤5% EaR
Mean Abs.	11.88	7.38	0.87	2.79
RMS	15.94	9.82	1.95	6.85
R^2	-0.48	-0.63	0.90	0.42

estimated value. The maximum power transfer method overestimates the *IE* by 11.88cal/cm^2 on average, while the mean error of the arc resistance method is 7.38cal/cm^2. There are a few cases where the arc resistance method underestimates the measured *IE*, roughly 1.5% of the tests in our dataset. The mean error of the median prediction of the self-extinguishing method is only 0.87cal/cm^2, however that is because roughly half (49%) of its predictions underestimate the *IE*. This is an improvement; however, we still do not want to underestimate the *IE* that a worker could be exposed to. The mean error of the $\leq 5\%$ chance, EaR prediction of the self-extinguishing method is 2.79cal/cm^2, with a 0.4% chance (1/228) of underestimating *IE* by more than 0.1cal/cm^2. A summary of these results divided up by arc flash PPE category is included in Table II. The maximum power method predicts a higher category than measured in 90% of tests. Compare that to the median self-extinguishing method correctly predicting the PPE category in 75% of tests. The $\leq 5\%$ EaR self-extinguishing method still predicts the correct PPE category in 61% of tests but reduces the rate of predicting a lower category from 11% to 0.4%. The improved performance of the self-extinguishing method is acute at low energy. Fig. 8 shows the *IE* of each test result plotted against the prediction of each method. Below 1.2cal/cm^2, the maximum power method and arc resistance method tend to overestimate the *IE* by one to two orders of magnitude. The proposed $\leq 5\%$ EaR self-extinguishing method is much better at correctly identifying when a test measures *IE* below this hazard threshold.

Additionally, the sensitivity of the proposed method to the tuning parameter beta is investigated. The following test case is used: 520 V battery, bolted fault current of 20 kA, and gap of 12.7 mm. To estimate sensitivity, beta is increased by 1% and the resulting change in the estimated arc time is recorded. For the test case with an inline configuration, a 1% increase in Beta causes a 12.97% increase in the median prediction of T_{arc} (1.19 s to 1.34 s), and a 2.6% increase in the $\leq 5\%$ chance prediction (3.88 s to 3.98 s). For the test case with an open parallel configuration, a 1% increase in Beta causes a 3.24% increase in in the median prediction of T_{arc} (0.0174 s to 0.0180 s) and a 6.06% increase in the $\leq 5\%$ chance prediction (0.0649 s to 0.0688 s). For the test case with a closed parallel configuration,

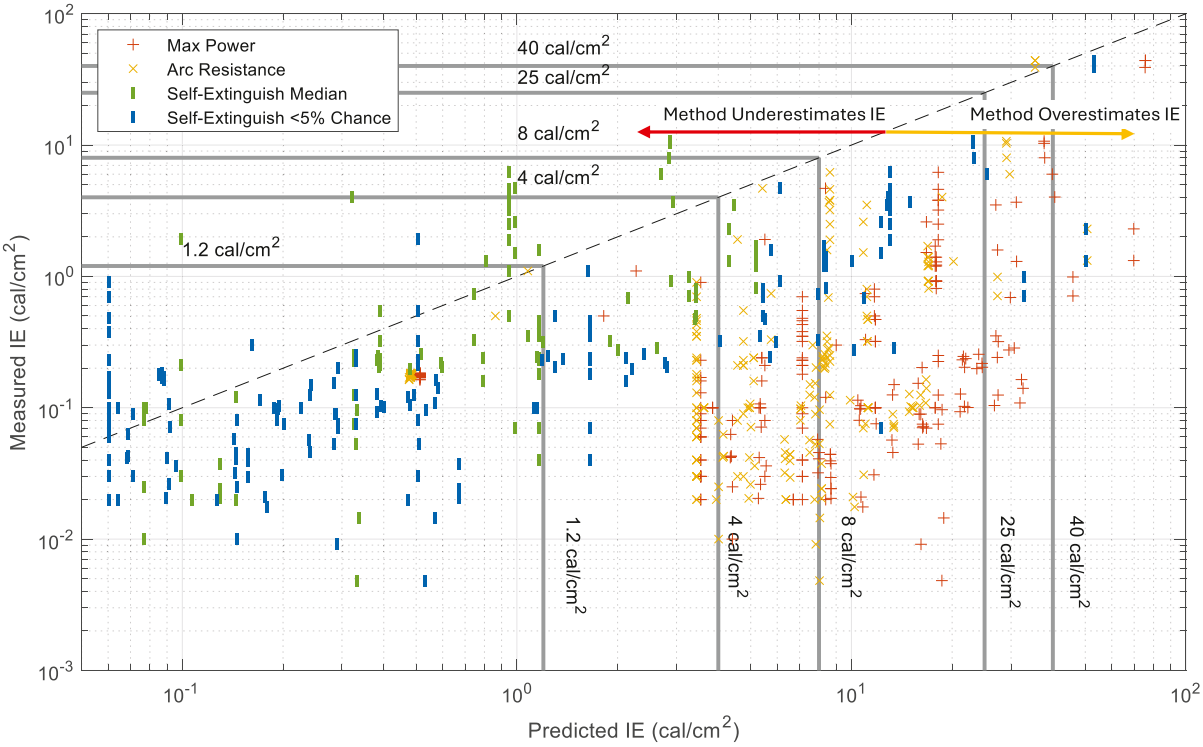


Fig. 8. Comparison of arc flash incident energy predictions and results.

a 1% increase in Beta causes a 5.4% increase in in the median prediction of T_{arc} (0.300 s to 0.316 s) and a 10.9% increase in the $\leq 5\%$ chance prediction (10.8 s to 12.0 s). These sensitivities are concerning because they imply that small changes in beta, perhaps from new experimental data being collected, could result in large changes in energy estimates.

There are several important caveats to keep in mind when reviewing these results. First, as previously stated the linear model used only applies to batteries (not PV, rectifiers, dc-generators) and only when working on or near the batteries themselves (low inductance circuits), when at rest (not under charge or discharge). Second, the probabilistic model does not fully account for the effect of arc current on the likelihood of self-extinguishing. It is understood that stronger magnetic forces should lead higher bolted fault current batteries to interrupt arcs more quickly. However, current has a more complex effect and we were unable to improve the predictive model by including current (bolted fault or initial arc current) or the resulting force in the model. More experimental data and better models may enable us to account for this in the future and improve our predictions further. This method should not be extended beyond the data used to train the beta tuning parameter. That means it is currently limited to less than 600 V for both inline and closed parallel configurations, and less than 1 kV for open parallel. Further, the open parallel configuration is limited to less than 10 kA short circuit current, while inline and closed parallel configurations are limited to less than 20 kA.

Lastly, as a probabilistic prediction, there will be outlier cases that have *IE* exposure greater than predicted by the model. For example, in the data presented in Fig. 8, there is one case where the $\leq$5% chance self-extinguishing model result predicted an *IE* of 0.5cal/cm^2 when the actual test measured approximately 2cal/cm^2. The source report included a surprising observation of this test "Review of high-speed video shows the arc grow substantially towards the calorimeter placed in front of the battery cabinet." We analyzed the current and voltage data from this test and determined that the higher *IE* measured was likely due to the effective working distance being reduced from 45.72 cm to roughly 30 cm. Outlier cases can and will happen and are one reason why PPE is the least effective method in the hierarchy of controls [3].

VI. Discussion on Selecting a Configuration

There are several factors to consider when selecting which configuration to use in the self-extinguishing calculation. First, while important to include for completeness, inline electrode configurations rarely if ever appear in battery systems. The exception is a split bus panel, with the feed for one bus coming from the opposite direction from the other. Every other dc panel is wired such that if an arc forms between busses, it is electromagnetically pushed to one end of the bus or the other until is either blocked by an insulating barrier or allowed to expand into open air. It is important to note that the dc loads fed by batteries tend to have some form of overcurrent protection that limit the duration of an arc more than self-extinguishing.

VII. Conclusion

Practical methods to estimate the arc flash hazard of battery systems are critical to keeping workers safe. This paper proposes a probabilistic, self-extinguishing arc model to predict arc duration. This method uses the battery voltage, short-circuit-current, arc gap, and the electrode configuration as inputs. These inputs are readily available to anyone with the battery specification sheet and a completed design or physical system to look at. Electrode configuration is generalized into three categories:

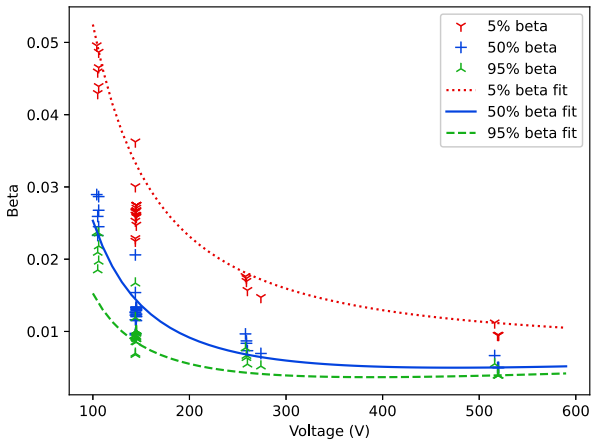


Fig. 9. Beta tuning parameterization for inline configurations.

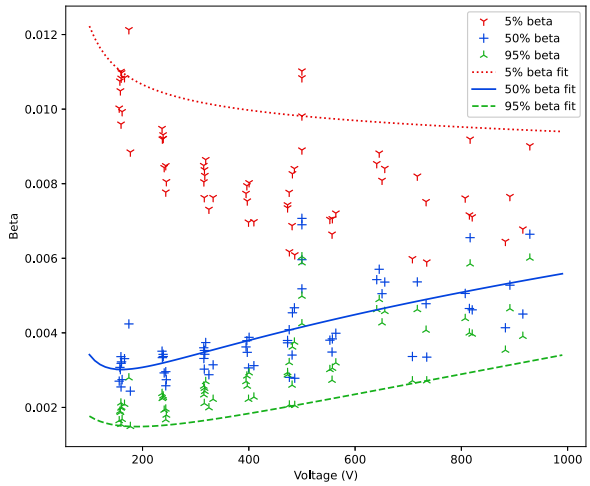


Fig. 10. Beta tuning parameterization for open parallel configurations

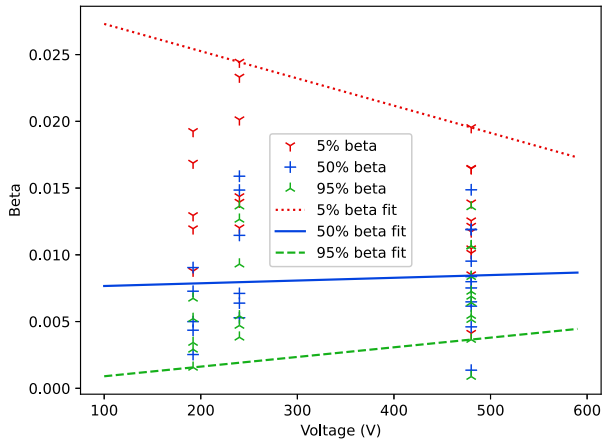


Fig. 11. Beta tuning parameterization for closed parallel configurations.

inline, open parallel, and closed parallel (terminated into an insulating barrier). For inline configurations, electrode erosion dominates the process of self-extinguishing, so current over time is used to predict the arc duration and final arc gap. In parallel configurations the process of self-extinguishing is dominated by the Lorentz forces. Terminating parallel conductors in an insulating boundary, such as a breaker, can greatly extend the duration of the arc and make the arc duration more random / less predictable.

The proposed methods are both practical, and more accurate than comparable methods. The self-extinguishing method, tuned to a $\leq 5\%$ EaR, has an average prediction error of 2.79cal/cm^2, compared to 11.88cal/cm^2 for the maximum power method and 7.38cal/cm^2 for the arc resistance method. This leads the EaR arc-extinguishing method to perform substantially better when it is used to select arc rated PPE, especially at low energy. This method correctly identifies the minimum category of PPE that would protect a worker 67% of tests, with 32% overestimating the required PPE and a $<1\%$ chance of underestimating it. This is a substantial improvement over the maximum power method which overestimates the required PPE in 89% of tests and the arc resistance method that overestimates the required PPE in 87% of tests. This improved accuracy will enable the correct selection of PPE for battery work, keeping workers safe while avoiding the hazards of excessive arc flash gear.

Future work will focus on improving calculation of the tuning parameter β. More experimental data in the closed parallel configuration could improve both accuracy and precision of the model.

Appendix
: Model Tuning

The tuning parameter β for inline configurations is calculated as a function of battery voltage as shown in Fig. 9. Of the 74 experiments, a subset of 38 were selected to train the parameter β for inline configurations. The best fit line with the data available was the sum of two power law functions as shown in (37).

$$\beta_{\text{inline}} = aV^b + cV^d \tag{37}$$

The tuning parameter β for open parallel configurations is calculated as a function of battery voltage as shown in Fig. 10. Of the 84 aggregated experiments, a subset of 65 were selected to train the parameter β for open parallel configurations. The best fit line with the data available was the sum of two power law functions as shown in (38).

$$\beta_{\text{open-parallel}} = aV^b + cV^d \tag{38}$$

The tuning parameter β for closed parallel configurations is calculated as a function of battery voltage as shown in Fig. 11. Of the 77 aggregated experiments, a subset of 22 were selected to train the parameter β for closed parallel configurations. The best fit line with the data available was a linear function as shown in (39).

$$\beta_{\text{closed-parallel}} = aV + b \tag{39}$$

A summary of the model parameters for each configuration is shown in Table III.

TABLE III
BETA FUNCTION PARAMETERS FOR (37), (38), AND (39)

	Median parameters $\beta_{50\%}$			
	a	b	c	d
Inline	46.62	-1.612	8.13E-6	0.9994
Open Parallel	13.29	-1.985	2.51E-4	0.4493
Closed Parallel	2.05E-6	7.46E-3	–	–

	$\leq$5% chance parameters $\beta_{5\%}$			
	a	b	c	d
Inline	50	-1.527	0.00781	-3.29E-6
Open Parallel	15.35	-1.999	0.01386	-0.05654
Closed Parallel	-2.04E-5	0.02934	–	–

ACKNOWLEDGMENT

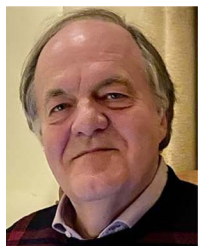
Sandia National Laboratories is a multi-mission laboratory managed and operated by National Technology & Engineering Solutions of Sandia, LLC (NTESS), a wholly owned subsidiary of Honeywell International Inc., for the U.S. Department of Energy's National Nuclear Security Administration (DOE/NNSA) under Contract DE-NA0003525. This written work is authored by an employee of NTESS. The employee, not NTESS, owns the right, title and interest in and to the written work and is responsible for its contents. Any subjective views or opinions that might be expressed in the written work do not necessarily represent the views of the U.S. Government. The publisher acknowledges that the U.S. Government retains a non-exclusive, paid-up, irrevocable, world-wide license to publish or reproduce the published form of this written work or allow others to do so, for U.S. Government purposes. The DOE will provide public access to results of federally sponsored research in accordance with the DOE Public Access Plan.

REFERENCES

[1] D. M. Rosewater, L. Gordon, and W. Cantor, "Practical battery arc flash models," in *Proc. IEEE IAS Elect. Saf. Workshop*, Mar. 2025, pp. 1–10, doi: 10.1109/ESW58401.2025.11159144.
[2] L. B. Gordon, L. Cartelli, and N. Graham, "A complete electrical shock hazard classification system and its application," *IEEE Trans. Ind. Appl.*, vol. 54, no. 6, pp. 6554–6565, Nov./Dec. 2018.
[3] "NFPA 70E 2024 Standardfor Electrical Safety in the Workplace, NFPA 70E, 2024.
[4] R. F. Ammerman, T. Gammon, P. K. Sen, and J. P. Nelson, "DC-arc models and incident-energy calculations," *IEEE Trans. Ind. Appl.*, vol. 46, no. 5, pp. 1810–1819, Sep./Oct. 2010.
[5] A. D. Stokes and W. T. Oppenlander, "Electric arcs in open air," *J. Phys. D: Appl. Phys.*, vol. 24, pp. 26–35, Apr. 1990.
[6] R. H. Lee, "The other electrical hazard: Electric arc blast burns," *IEEE Trans. Ind. Appl.*, vol. IA- 18, no. 3, pp. 246–251,May 1982.
[7] Battery hazard calculator (version 0.2), "Open Source Software," 2025. [Online]. Available: https://github.com/DavidRosewater/battery_arc_flash
[8] A. Marroquin and T. McKinch, "Methods for evaluating DC arc-flash incident energy in battery energy storage systems," in *Proc. 2023 IEEE IAS Elect. Saf. Workshop*, 2023, pp. 19–29.
[9] K. Gray, S. Robert, and T. Gauthier, "Low voltage 100–500 Vdc arc flash testing," in *Proc. IEEE IAS Elect. Saf. Workshop*, 2020, pp. 1–7.
[10] L. B. Gordon, "Modeling the dynamic behavior of DC arcs," *IEEE Trans. Ind. Appl.*, vol. 60, no. 1, pp. 1946–1955, Jan./Feb. 2024.
[11] K. Gray, S. Robert, and R. Hallé, "Sustainability of an electric arc flash at a voltage of 240 Vac and 150 Vdc," in *Proc. IEEE IAS Elect. Saf. Workshop*, Mar. 2023, pp. 1–6.
[12] W. Fechalos and P. Blake, "DC arc flash in stationary battery systems," in *Proc. Battcon Conf.*, May 2023, pp. 1–16.
[13] J. G. Hildreth and K. Feeney, "Arc flash hazards of 125 Vdc station battery systems," in *Proc. IEEE Power Energy Soc. Gen. Meeting* 2018, pp. 1–5.
[14] N. E. Jennings, D. A. Wetz, R. Langley, and J. M. Heinzel, "DC arc flash measurement from valve-regulated lead acid (VRLA) batteries," in *Proc. IEEE Electric Ship Technol. Symp.*, 2023, pp. 402–409.
[15] N. Jennings, D. Wetz, R. Langley, N. LaFlair, and J. Heinzel, "DC arc flash measurements from a 1000 V valve regulated lead acid battery system," *IEEE Open J. Ind. Appl.*, vol. 5, pp. 168–176, 2024.
[16] C. Ashton, "Modifying the DC arc-flash max power forumula to give more realistic predictions of maximum arc-flash energy," in *Proc. IEEE IAS Elect. Saf. Workshop*, 2024, pp. 1–7.
[17] W. Cantor, S. Marri, and L. Gordon, "NFPA 70E proposed DC arc flash updated guidance," in *Proc. IEEE IAS Elect. Saf. Workshop*, 2024, pp. 1–7, doi: 10.1109/ESW52258.2024.10752762.
[18] A. C. Gaunce et al., "DC arc flash: Testing and modeling incidents in a 125-V substation battery backup system," *IEEE Trans. Ind. Appl.*, vol. 56, no. 3, pp. 2138–2147, May/Jun. 2020.
[19] D. R. Doan, "Arc flash calculations for exposures to DC systems," *IEEE Trans. Ind. Appl.*, vol. 46, no. 6, pp. 2299–2302, Nov./Dec. 2010.
[20] T. Øyvang, E. Fjeld, W. Rondeel, and S. T. Hagen, "High current arc erosion on copper electrodes in air," in *Proc. IEEE 57th Holm Conf. Elect. Contacts*, 2011, pp. 1–6.
[21] W. E. Hart et al., *Pyomo–Optimization Modeling in Python*, vol. 67., 2nd ed. Cham, Switzerland: Springer, 2017.
[22] D. M. Rosewater, "Reducing risk when performing energized work on batteries," *IEEE Trans. Ind. Appl.*, vol. 60, no. 2, pp. 2732–2741, Mar./Apr. 2024.
[23] M. D. Fontaine and P. E. P. Walsh, "DC arc flash calculations — Arc-in-open-air and arc-in-a-box — Using a simplified approach (multiplication factor method)," in *Proc. IEEE IAS Elect. Saf. Workshop*, Daytona Beach, FL, 2012, pp. 1–8.



David Rosewater (Senior Member, IEEE) received the B.S. and M.S. degrees in electrical engineering from the Montana Tech of the University of Montana, Butte, MT, USA, and the Ph.D. degree in electrical and computer engineering from the University of Texas, Austin, TX, USA. He is currently a Grid Energy Storage Researcher with Sandia National Laboratories, Albuquerque, NM, USA. His research focuses on all aspects of integrating batteries into the power grid, such as safety, technology standards, modeling, control, and economics.



Lloyd B. Gordon (Life Senior Member, IEEE) received the Ph.D. degree in electrical engineering from Texas Tech University, Lubbock, TX, USA, in 1981. From 1981 to 1986, he started his research career with Lawrence Livermore National Laboratory (DOE), conducting research in topics of pulsed power engineering, plasma physics, and dielectric engineering. From 1986 to 1991, he was with the Department of Electrical Engineering, Auburn University, Auburn, AL, USA, and with the Department of Electrical Engineering, University of Texas, Arlington, TX, USA, from 1991 to 1998. From 1998 to 2021, he was with Los Alamos National Laboratory (DOE). He has 25 years of experience in experimental high-energy research, 45 years of experience as an educator and trainer, and has focused his efforts on R&D of electrical safety for more than past 25 years. He has lectured to and trained more than 100 000 scientists and engineers throughout the DOE, DOD, NASA, and industry more than the past 35 years in R&D Electrical Safety. He is on the NFPA 70E, Chapter three task group, and Guide to Arc Flash Calculations. He has been a member for 52 years.



William Cantor (Senior Member, IEEE) received the B.S. degree in chemical engineering and the M.S. degree in electrical engineering. He is currently an Assistant Teaching Professor with the Pennsylvania State University, University Park, PA, USA. He has more than 30 years' experience in the stationary battery industry and has been an Active Participant in the development of related IEEE Standards and Active Member of IEEE PES ESSB committee. He represents IEEE PES/IAS on various NFPA committees.